ELSEVIER

SCIENCE DIRECT®

Physics Letters B 561 (2003) 73–81

PHYSICS LETTERS B

www.elsevier.com/locate/npe

Study of the $e^+e^- \to Ze^+e^-$ process at LEP

L3 Collaboration

P. Achard [t], O. Adriani [q], M. Aguilar-Benitez [x], J. Alcaraz [x,r], G. Alemanni [v], J. Allaby [r], A. Aloisio [ab], M.G. Alviggi [ab], H. Anderhub [at], V.P. Andreev [f,ag], F. Anselmo [h], A. Arefiev [aa], T. Azemoon [c], T. Aziz [i,r], P. Bagnaia [al], A. Bajo [x], G. Baksay [y], L. Baksay [y], S.V. Baldew [b], S. Banerjee [i], Sw. Banerjee [d], A. Barczyk [at,ar], R. Barillère [r], P. Bartalini [v], M. Basile [h], N. Batalova [aq], R. Battiston [af], A. Bay [v], F. Becattini [q], U. Becker [m], F. Behner [at], L. Bellucci [q], R. Berbeco [c], J. Berdugo [x], P. Berges [m], B. Bertucci [af], B.L. Betev [at], M. Biasini [af], M. Biglietti [ab], A. Biland [at], J.J. Blaising [d], S.C. Blyth [ah], G.J. Bobbink [b], A. Böhm [a], L. Boldizsar [l], B. Borgia [al], S. Bottai [q], D. Bourilkov [at], M. Bourquin [t], S. Braccini [t], J.G. Branson [an], F. Brochu [d], J.D. Burger [m], W.J. Burger [af], X.D. Cai [m], M. Capell [m], G. Cara Romeo [h], G. Carlino [ab], A. Cartacci [q], J. Casaus [x], F. Cavallari [al], N. Cavallo [ai], C. Cecchi [af], M. Cerrada [x], M. Chamizo [t], Y.H. Chang [av], M. Chemarin [w], A. Chen [av], G. Chen [g], G.M. Chen [g], H.F. Chen [u], H.S. Chen [g], G. Chiefari [ab], L. Cifarelli [am], F. Cindolo [h], I. Clare [m], R. Clare [ak], G. Coignet [d], N. Colino [x], S. Costantini [al], B. de la Cruz [x], S. Cucciarelli [af], J.A. van Dalen [ad], R. de Asmundis [ab], P. Déglon [t], J. Debreczeni [l], A. Degré [d], K. Dehmelt [y], K. Deiters [ar], D. della Volpe [ab], E. Delmeire [t], P. Denes [aj], F. DeNotaristefani [al], A. De Salvo [at], M. Diemoz [al], M. Dierckxsens [b], C. Dionisi [al], M. Dittmar [at,r], A. Doria [ab], M.T. Dova [j,5], D. Duchesneau [d], M. Duda [a], B. Echenard [t], A. Eline [r], A. El Hage [a], H. El Mamouni [w], A. Engler [ah], F.J. Eppling [m], P. Extermann [t], M.A. Falagan [x], S. Falciano [al], A. Favara [ae], J. Fay [w], O. Fedin [ag], M. Felcini [at], T. Ferguson [ah], H. Fesefeldt [a], E. Fiandrini [af], J.H. Field [t], F. Filthaut [ad], P.H. Fisher [m], W. Fisher [aj], I. Fisk [an], G. Forconi [m], K. Freudenreich [at], C. Furetta [z], Yu. Galaktionov [aa,m], S.N. Ganguli [i], P. Garcia-Abia [e,r], M. Gataullin [ae], S. Gentile [al], S. Giagu [al], Z.F. Gong [u], G. Grenier [w], O. Grimm [at], M.W. Gruenewald [p], M. Guida [am], R. van Gulik [b], V.K. Gupta [aj], A. Gurtu [i], L.J. Gutay [aq], D. Haas [e], R.Sh. Hakobyan [ad], D. Hatzifotiadou [h], T. Hebbeker [a], A. Hervé [r], J. Hirschfelder [ah], H. Hofer [at], M. Hohlmann [y], G. Holzner [at], S.R. Hou [av], Y. Hu [ad], B.N. Jin [g], L.W. Jones [c], P. de Jong [b], I. Josa-Mutuberría [x], D. Käfer [a], M. Kaur [n], M.N. Kienzle-Focacci [t], J.K. Kim [ap], J. Kirkby [r], W. Kittel [ad], A. Klimentov [m,aa], A.C. König [ad], M. Kopal [aq], V. Koutsenko [m,aa], M. Kräber [at], R.W. Kraemer [ah],

0370-2693
doi:10.1016/S0370-2693(03)00406-4

A. Krüger [as], A. Kunin [m], P. Ladron de Guevara [x], I. Laktineh [w], G. Landi [q], M. Lebeau [r], A. Lebedev [m], P. Lebrun [w], P. Lecomte [at], P. Lecoq [r], P. Le Coultre [at], J.M. Le Goff [r], R. Leiste [as], M. Levtchenko [z], P. Levtchenko [ag], C. Li [u], S. Likhoded [as], C.H. Lin [av], W.T. Lin [av], F.L. Linde [b], L. Lista [ab], Z.A. Liu [g], W. Lohmann [as], E. Longo [al], Y.S. Lu [g], C. Luci [al], L. Luminari [al], W. Lustermann [at], W.G. Ma [u], L. Malgeri [t], A. Malinin [aa], C. Maña [x], D. Mangeol [ad], J. Mans [aj], J.P. Martin [w], F. Marzano [al], K. Mazumdar [i], R.R. McNeil [f], S. Mele [r,ab], L. Merola [ab], M. Meschini [q], W.J. Metzger [ad], A. Mihul [k], H. Milcent [r], G. Mirabelli [al], J. Mnich [a], G.B. Mohanty [i], G.S. Muanza [w], A.J.M. Muijs [b], B. Musicar [an], M. Musy [al], S. Nagy [o], S. Natale [t], M. Napolitano [ab], F. Nessi-Tedaldi [at], H. Newman [ae], A. Nisati [al], H. Nowak [as], R. Ofierzynski [at], G. Organtini [al], C. Palomares [r], P. Paolucci [ab], R. Paramatti [al], G. Passaleva [q], S. Patricelli [ab], T. Paul [j], M. Pauluzzi [af], C. Paus [m], F. Pauss [at], M. Pedace [al], S. Pensotti [z], D. Perret-Gallix [d], B. Petersen [ad], D. Piccolo [ab], F. Pierella [h], M. Pioppi [af], P.A. Piroué [aj], E. Pistolesi [z], V. Plyaskin [aa], M. Pohl [t], V. Pojidaev [q], J. Pothier [r], D.O. Prokofiev [aq], D. Prokofiev [ag], J. Quartieri [am], G. Rahal-Callot [at], M.A. Rahaman [i], P. Raics [o], N. Raja [i], R. Ramelli [at], P.G. Rancoita [z], R. Ranieri [q], A. Raspereza [as], P. Razis [ac], D. Ren [at], M. Rescigno [al], S. Reucroft [j], S. Riemann [as], K. Riles [c], B.P. Roe [c], L. Romero [x], A. Rosca [as], S. Rosier-Lees [d], S. Roth [a], C. Rosenbleck [a], B. Roux [ad], J.A. Rubio [r], G. Ruggiero [q], H. Rykaczewski [at], A. Sakharov [at], S. Saremi [f], S. Sarkar [al], J. Salicio [r], E. Sanchez [x], M.P. Sanders [ad], C. Schäfer [r], V. Schegelsky [ag], H. Schopper [au], D.J. Schotanus [ad], C. Sciacca [ab], L. Servoli [af], S. Shevchenko [ae], N. Shivarov [ao], V. Shoutko [m], E. Shumilov [aa], A. Shvorob [ae], D. Son [ap], C. Souga [w], P. Spillantini [q], M. Steuer [m], D.P. Stickland [aj], B. Stoyanov [ao], A. Straessner [r], K. Sudhakar [i], G. Sultanov [ao], L.Z. Sun [u], S. Sushkov [a], H. Suter [at], J.D. Swain [j], Z. Szillasi [y,3], X.W. Tang [g], P. Tarjan [o], L. Tauscher [e], L. Taylor [j], B. Tellili [w], D. Teyssier [w], C. Timmermans [ad], Samuel C.C. Ting [m], S.M. Ting [m], S.C. Tonwar [i,r], J. Tóth [l], C. Tully [aj], K.L. Tung [g], J. Ulbricht [at], E. Valente [al], R.T. Van de Walle [ad], R. Vasquez [aq], V. Veszpremi [y], G. Vesztergombi [l], I. Vetlitsky [aa], D. Vicinanza [am], G. Viertel [at], S. Villa [ak], M. Vivargent [d], S. Vlachos [e], I. Vodopianov [y], H. Vogel [ah], H. Vogt [as], I. Vorobiev [ah,aa], A.A. Vorobyov [ag], M. Wadhwa [e], X.L. Wang [u], Z.M. Wang [u], M. Weber [a], P. Wienemann [a], H. Wilkens [ad], S. Wynhoff [aj], L. Xia [ae], Z.Z. Xu [u], J. Yamamoto [c], B.Z. Yang [u], C.G. Yang [g], H.J. Yang [c], M. Yang [g], S.C. Yeh [aw], An. Zalite [ag], Yu. Zalite [ag], Z.P. Zhang [u], J. Zhao [u], G.Y. Zhu [g], R.Y. Zhu [ae], H.L. Zhuang [g], A. Zichichi [h,r,s], B. Zimmermann [at], M. Zöller [a]

[a] *III. Physikalisches Institut, RWTH, D-52056 Aachen, Germany* [1]
[b] *National Institute for High Energy Physics, NIKHEF, and University of Amsterdam, NL-1009 DB Amsterdam, The Netherlands*
[c] *University of Michigan, Ann Arbor, MI 48109, USA*
[d] *Laboratoire d'Annecy-le-Vieux de Physique des Particules, LAPP, IN2P3-CNRS, BP 110, F-74941 Annecy-le-Vieux cedex, France*
[e] *Institute of Physics, University of Basel, CH-4056 Basel, Switzerland*
[f] *Louisiana State University, Baton Rouge, LA 70803, USA*
[g] *Institute of High Energy Physics, IHEP, 100039 Beijing, China* [6]

[h] University of Bologna and INFN-Sezione di Bologna, I-40126 Bologna, Italy
[i] Tata Institute of Fundamental Research, Mumbai (Bombay) 400 005, India
[j] Northeastern University, Boston, MA 02115, USA
[k] Institute of Atomic Physics and University of Bucharest, R-76900 Bucharest, Romania
[l] Central Research Institute for Physics of the Hungarian Academy of Sciences, H-1525 Budapest 114, Hungary [2]
[m] Massachusetts Institute of Technology, Cambridge, MA 02139, USA
[n] Panjab University, Chandigarh 160 014, India
[o] KLTE-ATOMKI, H-4010 Debrecen, Hungary [3]
[p] Department of Experimental Physics, University College Dublin, Belfield, Dublin 4, Ireland
[q] INFN Sezione di Firenze and University of Florence, I-50125 Florence, Italy
[r] European Laboratory for Particle Physics, CERN, CH-1211 Geneva 23, Switzerland
[s] World Laboratory, FBLJA Project, CH-1211 Geneva 23, Switzerland
[t] University of Geneva, CH-1211 Geneva 4, Switzerland
[u] Chinese University of Science and Technology, USTC, Hefei, Anhui 230 029, China [6]
[v] University of Lausanne, CH-1015 Lausanne, Switzerland
[w] Institut de Physique Nucléaire de Lyon, IN2P3-CNRS, Université Claude Bernard, F-69622 Villeurbanne, France
[x] Centro de Investigaciones Energéticas, Medioambientales y Tecnológicas, CIEMAT, E-28040 Madrid, Spain [4]
[y] Florida Institute of Technology, Melbourne, FL 32901, USA
[z] INFN-Sezione di Milano, I-20133 Milan, Italy
[aa] Institute of Theoretical and Experimental Physics, ITEP, Moscow, Russia
[ab] INFN-Sezione di Napoli and University of Naples, I-80125 Naples, Italy
[ac] Department of Physics, University of Cyprus, Nicosia, Cyprus
[ad] University of Nijmegen and NIKHEF, NL-6525 ED Nijmegen, The Netherlands
[ae] California Institute of Technology, Pasadena, CA 91125, USA
[af] INFN-Sezione di Perugia and Università Degli Studi di Perugia, I-06100 Perugia, Italy
[ag] Nuclear Physics Institute, St. Petersburg, Russia
[ah] Carnegie Mellon University, Pittsburgh, PA 15213, USA
[ai] INFN-Sezione di Napoli and University of Potenza, I-85100 Potenza, Italy
[aj] Princeton University, Princeton, NJ 08544, USA
[ak] University of Californa, Riverside, CA 92521, USA
[al] INFN-Sezione di Roma and University of Rome, "La Sapienza", I-00185 Rome, Italy
[am] University and INFN, Salerno, I-84100 Salerno, Italy
[an] University of California, San Diego, CA 92093, USA
[ao] Bulgarian Academy of Sciences, Central Lab. of Mechatronics and Instrumentation, BU-1113 Sofia, Bulgaria
[ap] The Center for High Energy Physics, Kyungpook National University, 702-701 Taegu, South Korea
[aq] Purdue University, West Lafayette, IN 47907, USA
[ar] Paul Scherrer Institut, PSI, CH-5232 Villigen, Switzerland
[as] DESY, D-15738 Zeuthen, Germany
[at] Eidgenössische Technische Hochschule, ETH Zürich, CH-8093 Zürich, Switzerland
[au] University of Hamburg, D-22761 Hamburg, Germany
[av] National Central University, Chung-Li, Taiwan
[aw] Department of Physics, National Tsing Hua University, Taiwan

Received 2 December 2002; received in revised form 13 March 2003; accepted 18 March 2003

Editor: L. Rolandi

Abstract

The cross section of the process $e^+e^- \to Ze^+e^-$ is measured with 0.7 fb^{-1} of data collected with the L3 detector at LEP. Decays of the Z boson into quarks and muons are considered at centre-of-mass energies ranging from 183 GeV up to 209 GeV. The measurements are found to agree with Standard Model predictions, achieving a precision of about 10% for the hadronic channel.

1. Introduction

The study of gauge boson production in e^+e^- collisions constitutes one of the main subjects of the scientific program carried out at LEP. Above the Z resonance, in addition to the s- and t-channel pair-production processes, "single" weak gauge bosons can also be produced via t-channel processes. A common feature of this single boson production is the emission of a virtual photon off the incoming electron or positron. This electron or positron remains in turn almost unscattered at very low polar angles and hence not detected. Particular care has to be paid when predicting the cross sections of these processes due to the running of the electromagnetic coupling of the photon and the peculiarities of the modelling of small angle scattering. The comparison of these predictions with experimental data is made more interesting by the fact that single boson production will constitute a copious source of bosons at higher-energy e^+e^- colliders. In addition, this process constitutes a significant background for the search of Standard Model Higgs boson or new particles predicted in physics beyond the Standard Model. The "single W" production is extensively studied at LEP [1,2] and this Letter concentrates on "single Z" production. Results at lower centre-of-mass energies were previously reported [1,3].

Fig. 1 presents two Feynman diagrams for the single Z production, followed by the decay of the Z into a quark–antiquark or a muon–antimuon pair. A distinctive feature of this process is the photon–electron scattering, reminiscent of the Compton scattering. These diagrams are only an example of the 48 diagrams contributing to the $e^+e^- \to q\bar{q}e^+e^-$ and $e^+e^- \to \mu^+\mu^-e^+e^-$ final state processes. The single Z signal is defined starting from this full set of diagrams. QCD contributions from two-photon physics with $e^+e^- \to q\bar{q}e^+e^-$ final state are not considered. The definition requires the final state fermions to satisfy the kinematical cuts:

$$m_{f\bar{f}} > 60\ \text{GeV}, \qquad \theta_{\text{unscattered}} < 12^\circ,$$
$$60^\circ < \theta_{\text{scattered}} < 168^\circ, \qquad E_{\text{scattered}} > 3.0\ \text{GeV}, \quad (1)$$

where $m_{f\bar{f}}$ refers to the invariant mass of the produced quark–antiquark or muon–antimuon pair, $\theta_{\text{unscattered}}$ is the polar angle at which the electron[7] closest to the beam line is emitted, $\theta_{\text{scattered}}$ and $E_{\text{scattered}}$ are respectively the polar angle with respect to its incoming direction and the energy of the electron scattered at the largest polar angle.

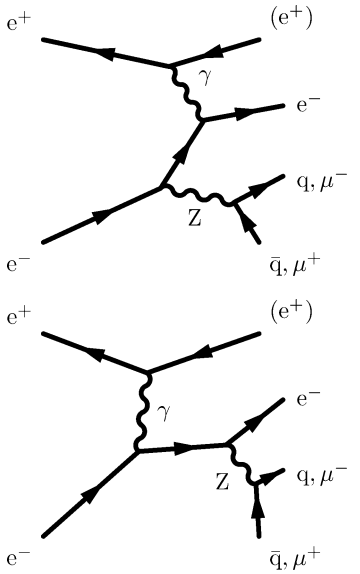

Fig. 1. Main diagrams contributing to the "single Z" production.

These criteria largely enhance the contribution of diagrams similar to those in Fig. 1 over the remaining phase space of the $e^+e^- \to q\bar{q}e^+e^-$ and $e^+e^- \to \mu^+\mu^-e^+e^-$ processes and correspond to predicted cross sections at a centre-of-mass energy $\sqrt{s} = 200$ GeV of about 0.6 pb for the hadron channel and of about 0.04 pb for the muon one. The most severe backgrounds for the detection of the single Z production at LEP are the $e^+e^- \to q\bar{q}(\gamma)$ and the $e^+e^- \to \mu^+\mu^-(\gamma)$ processes, for the hadron and muon channels, respectively.

[1] Supported by the German Bundesministerium für Bildung, Wissenschaft, Forschung und Technologie.

[2] Supported by the Hungarian OTKA fund under contract Nos. T019181, F023259 and T037350.

[3] Also supported by the Hungarian OTKA fund under contract No. T026178.

[4] Supported also by the Comisión Interministerial de Ciencia y Tecnología.

[5] Also supported by CONICET and Universidad Nacional de La Plata, CC 67, 1900 La Plata, Argentina.

[6] Supported by the National Natural Science Foundation of China.

[7] The word "electron" is used for both electrons and positrons.

This Letter describes the selection of $e^+e^- \to Ze^+e^- \to q\bar{q}e^+e^-$ and $e^+e^- \to Ze^+e^- \to \mu^+\mu^-e^+e^-$ events in the data sample collected by the L3 detector [4] at LEP and the measurement of the cross section of these processes.

2. Data and Monte Carlo samples

This analysis is based on 675.5 pb^{-1} of integrated luminosity collected at $\sqrt{s} = 182.7$–209.0 GeV. For the investigation of the $e^+e^- \to Ze^+e^- \to q\bar{q}e^+e^-$ channel, this sample is divided into eight different energy bins whose corresponding average $\sqrt{s}$ values and integrated luminosities are reported in Table 1.

The signal process is modelled with the WPHACT Monte Carlo program [5]. The GRC4F [6] event generator is used for systematic checks. Events are generated in a phase space broader than the one defined by the criteria (1). Those events who do not satisfy these criteria are considered as background. The $e^+e^- \to q\bar{q}(\gamma)$, $e^+e^- \to \mu^+\mu^-(\gamma)$ and $e^+e^- \to \tau^-\tau^+(\gamma)$ processes are simulated with the KK2f [7] Monte Carlo generator, the $e^+e^- \to ZZ$ process with PYTHIA [8], and the $e^+e^- \to W^+W^-$ process, with the exception of the $q\bar{q}'e\nu$ final state, with KORALW [9]. EXCALIBUR [10] is used to simulate the $q\bar{q}'e\nu$ and other four-fermion final states. Hadron and lepton production in two-photon interactions are modelled with PHOJET [11] and DIAG36 [12], respectively. The generated events are passed through the L3 detector simulation program [13]. Time dependent detector inefficiencies, as monitored during the data taking period, are also simulated.

3. Event selection

3.1. $e^+e^- \to Ze^+e^- \to q\bar{q}e^+e^-$ channel

The selection of events in the $e^+e^- \to Ze^+e^- \to q\bar{q}e^+e^-$ channel proceeds from high multiplicity events with at least one electron identified in the BGO electromagnetic calorimeter and in the central tracker with an energy above 3 GeV. Electron isolation criteria are applied. These are based on the energy deposition and track multiplicity around the electron candidate.

To strongly suppress the contribution from the high cross section background processes, the signal topology is enforced requiring events with a reconstructed invariant mass of the hadronic system, stemming from a Z boson, between 50 and 130 GeV, a visible energy of at least $0.40\sqrt{s}$ and a missing momentum, due to the undetected electron, of at least $0.24\sqrt{s}$. These quantities are computed from charged tracks, calorimetric clusters and possible muons. After these selection criteria, 1551 events are selected in the full data sample. From Monte Carlo, 1551 ± 4 events are expected, out of which 208 ± 1 are signal events, selected with an efficiency of 54%. Most of the background arises from the $e^+e^- \to q\bar{q}'e\nu$ (58%), $e^+e^- \to q\bar{q}(\gamma)$ (19%) and $e^+e^- \to W^+W^-$ (11%) processes.

The particular signature of an electron undetected at low angle and the other scattered in the detector, allows to reject a large fraction of the background by considering two powerful kinematic variables: the product of the charge, q, of the detected electron and the cosine of its polar angle measured with respect to the direction of the incoming electron, $\cos\theta$, and the product of q and the polar angle of the direction of the missing momentum, $\cos\phi$. Two selection criteria are applied:

$$q\cos\theta > -0.5 \quad \text{and} \quad q\cos\phi > 0.94.$$

Distributions of these variables are presented in Fig. 2. In addition, events are forced into two jets by means of the DURHAM algorithm [14], and the opening angle between the two jets in the plane transverse to the beam direction is required to exceed 150°. The selected electrons are not considered when forming those jets. Background events are further rejected by tightening the electron isolation criteria. Table 2 summarises the yield of this event selection.

Table 1
The average centre-of-mass energies and the corresponding integrated luminosities of the data sample used in this study

$\sqrt{s}$ [GeV]	182.7	188.6	191.6	195.5	199.5	201.7	204.9	206.6
$\mathcal{L}$ [pb^{-1}]	55.1	176.0	29.4	83.0	80.8	36.7	76.6	137.9

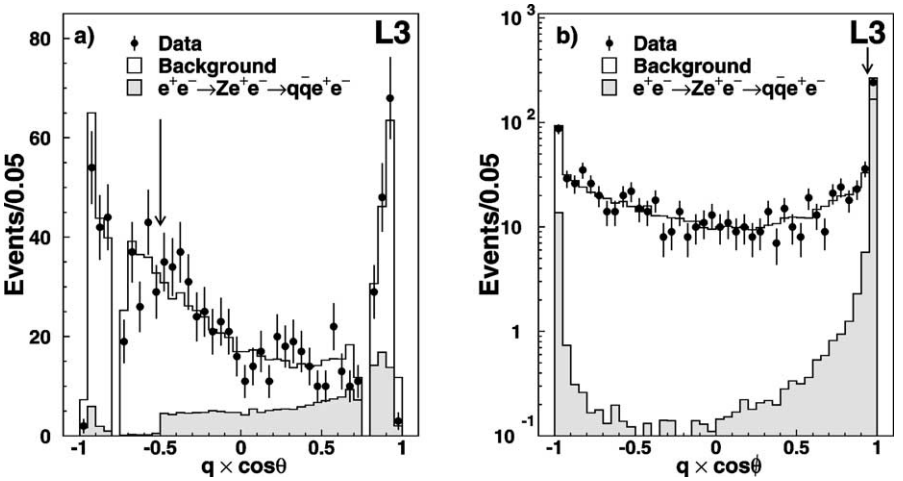

Fig. 2. Distributions for data, signal and background Monte Carlo of the product of the charge of the detected electron and (a) the cosine of its polar angle and (b) the cosine of the polar angle of the missing momentum. The arrows show the position of the applied cuts. All other selection criteria but those on these two variables are applied. Signal events around -1 correspond to charge confusion in the central tracker. The sharp edge of the signal distribution in (a) at -0.5 follows from the signal definition criterion $\theta_{\text{scattered}} > 60^\circ$; moreover, the depletion around ± 0.7 in data and Monte Carlo is due to the absence of the BGO calorimeter in this angular region.

Table 2
Yield of the $e^+e^- \to Ze^+e^- \to q\bar{q}e^+e^-$ event selection at the different centre-of-mass energies

$\sqrt{s}$ [GeV]	ε [%]	N_{Data}	N_{MC}	N_{Sign}	$N_{q\bar{q}(\gamma)}$	$N_{q\bar{q}'e\nu}$	$N_{\text{two-phot}}$
182.7	42.3	16	16.0 ± 0.5	12.0 ± 0.2	3.2	0.4	0.2
188.6	42.7	53	52.4 ± 1.2	40.3 ± 0.6	9.5	0.5	1.0
191.6	43.0	9	8.7 ± 0.3	6.9 ± 0.2	1.3	0.0	0.3
195.5	45.0	19	26.5 ± 0.6	21.2 ± 0.3	3.6	0.0	1.1
199.5	45.2	18	27.1 ± 0.7	21.3 ± 0.3	3.8	0.4	1.2
201.7	44.0	16	12.2 ± 0.5	9.5 ± 0.2	1.6	0.3	0.5
204.9	43.3	24	24.6 ± 0.4	19.9 ± 0.3	2.9	0.2	1.1
206.6	44.6	47	46.2 ± 0.7	37.2 ± 0.6	5.4	0.3	2.2

The signal efficiency, ε, is listed together with the number of observed, N_{Data}, and total expected, N_{MC}, events. The expected number of signal events, N_{Sign}, is given together with details of the most important residual backgrounds, respectively indicated with $N_{q\bar{q}(\gamma)}$, $N_{q\bar{q}'e\nu}$ and $N_{\text{two-phot}}$ for the processes $e^+e^- \to q\bar{q}(\gamma)$, $e^+e^- \to q\bar{q}'e\nu$ and hadron production in two-photon interactions.

3.2. $e^+e^- \to Ze^+e^- \to \mu^+\mu^-e^+e^-$ *channel*

Candidates for the $e^+e^- \to Ze^+e^- \to \mu^+\mu^-e^+e^-$ process are selected by first requiring low multiplicity events with three tracks in the central tracker, corresponding to one electron with energy above 3 GeV and two muons, reconstructed in the muon spectrometer with momenta above 18 GeV. A kinematic fit is then applied which requires momentum conservation in the plane transverse to the beam axis. The reconstructed invariant mass of the two muons should lie between 55 and 145 GeV. Finally, three additional selection criteria are applied:

$$-0.50 < q\cos\theta < 0.93,$$

$$q\cos\phi > 0.50 \quad \text{and} \quad q\cos\theta_{\text{Z}} < 0.40,$$

where $\cos\theta_{\text{Z}}$ is the polar angle of the Z boson as reconstructed from the two muons. These criteria select 9 data events and 6.6 ± 0.1 expected events from signal Monte Carlo with an efficiency of 22%. Background expectations amount to 1.5 ± 0.1 events, coming in equal parts from muon-pair production in two-photon interactions, the $e^+e^- \to \mu^+\mu^-(\gamma)$

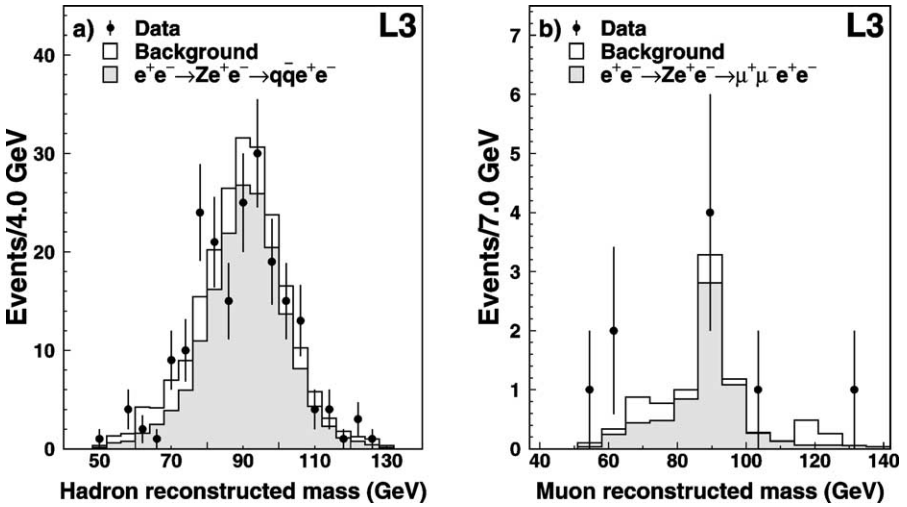

Fig. 3. Distribution of the reconstructed invariant mass of (a) the hadron system and (b) the muon system for data, signal, and background Monte Carlo events.

process, and $e^+e^- \to \mu^+\mu^-e^+e^-$ events generated with WPHACT that do not pass the signal definition criteria.

4. Results

Fig. 3(a) presents the distribution of the invariant mass of the hadronic system after applying all selection criteria of the $e^+e^- \to Ze^+e^- \to q\bar{q}e^+e^-$ channel. A large signal peaking around the mass of the Z boson is observed. The single Z cross section at each value of $\sqrt{s}$ is determined from a maximum-likelihood fit to the distribution of this variable. The results are listed in Table 3, together with the predictions of the WPHACT Monte Carlo. A good agreement is observed.

The invariant mass of muon pairs from the $e^+e^- \to Ze^+e^- \to \mu^+\mu^-e^+e^-$ selected events is shown in Fig. 3(b). The cross section of this process is determined with a fit to the invariant mass distribution, over the full data sample, as:

$$\sigma\left(e^+e^- \to Ze^+e^- \to \mu^+\mu^-e^+e^-\right) = 0.043^{+0.013}_{-0.013} \pm 0.003\ \text{pb} \quad \left(\sigma^{\text{SM}} = 0.044\ \text{pb}\right),$$

where the first uncertainty is statistical and the second systematic. This measurement agrees with the Standard Model prediction σ^{SM} reported in parenthesis, which is calculated with the WPHACT program as the luminosity weighted average cross section over the different centre-of-mass energies.

Table 3
Measured and expected cross sections for the $e^+e^- \to Ze^+e^- \to q\bar{q}e^+e^-$ process at the different centre-of-mass energies

$\sqrt{s}$ [GeV]	σ^{Measured} [pb]	σ^{Expected} [pb]
182.7	$0.51^{+0.19}_{-0.16} \pm 0.03$	0.51
188.6	$0.54^{+0.10}_{-0.09} \pm 0.03$	0.54
191.6	$0.60^{+0.26}_{-0.21} \pm 0.04$	0.55
195.5	$0.40^{+0.13}_{-0.11} \pm 0.02$	0.56
199.5	$0.33^{+0.12}_{-0.10} \pm 0.02$	0.58
201.7	$0.81^{+0.26}_{-0.22} \pm 0.05$	0.59
204.9	$0.55^{+0.16}_{-0.14} \pm 0.03$	0.60
206.6	$0.59^{+0.12}_{-0.10} \pm 0.03$	0.61

The first uncertainties are statistical and the second systematic. Expectations are calculated with the WPHACT Monte Carlo program.

Several possible sources of systematic uncertainty are considered and their effects on the measured cross sections are listed in Table 4. First, detector effects and the accuracy of the Monte Carlo simulations are investigated by varying the energy scale of the calorimeters, the amount of charge confusion in the tracker, visible for instance in Fig. 2 as the signal enhancement on the left side, and the selection criteria. The impact of the signal modelling on the final efficiencies is stud-

Table 4
Sources of systematic uncertainties

Source	Systematic uncertainty	
	$e^+e^- \to Ze^+e^- \to q\bar{q}e^+e^-$ (%)	$e^+e^- \to Ze^+e^- \to \mu^+\mu^-e^+e^-$ (%)
Energy scale	2.3	6.3
Charge confusion	0.8	< 0.1
Selection procedure	4.0	1.9
Signal modelling	1.2	< 0.1
Background modelling	1.0	2.9
Background Monte Carlo statistics	2.8	1.8
Signal Monte Carlo statistics	1.6	2.2
Total	5.9	7.7

ied by using the GRC4F Monte Carlo program instead of the WPHACT event generator to derive the signal efficiencies. The expected cross sections of the background processes for the $e^+e^- \to Ze^+e^- \to q\bar{q}e^+e^-$ channel are varied by 5% for $e^+e^- \to q\bar{q}(\gamma)$, 10% for $e^+e^- \to q\bar{q}'e\nu$, 1% for $e^+e^- \to W^+W^-$, and 50% for hadron production in two-photon interactions. The cross sections of the background processes for the $e^+e^- \to Ze^+e^- \to \mu^+\mu^-e^+e^-$ channel are varied by 2% for the $e^+e^- \to \mu^+\mu^-(\gamma)$ channel, 10% for the WPHACT $e^+e^- \to \mu^+\mu^-e^+e^-$ events that do not pass the signal definition and 25% for muon-pair production in two-photon interactions. Finally, the effects of the limited background and signal Monte Carlo statistics are considered. Fig. 4 compares the results of the measurement of the cross section of the process $e^+e^- \to Ze^+e^- \to q\bar{q}e^+e^-$ with both the WPHACT and the GRC4F predictions. A good agreement is observed. This agreement is quantified by extracting the ratio R between the measured cross sections σ^{Measured} and the WPHACT predictions σ^{Expected}:

$$R = \frac{\sigma^{\text{Measured}}}{\sigma^{\text{Expected}}} = 0.88 \pm 0.08 \pm 0.06,$$

where the first uncertainty is statistical and the second systematic.

In conclusion, the process $e^+e^- \to Ze^+e^-$ has been observed at LEP for decays of the Z boson into both hadrons and muons. The measured cross sections have been compared with the Standard Model predictions, and were found in agreement with an experimental accuracy of about 10% for decays of the Z boson into hadrons.

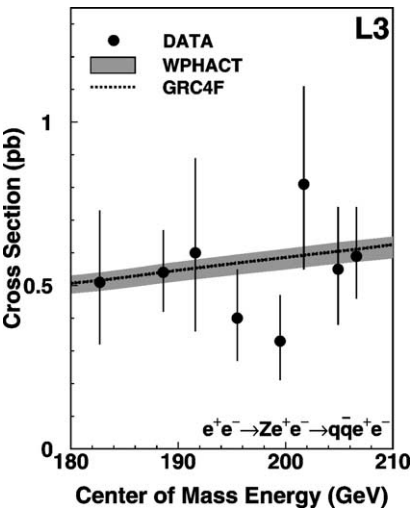

Fig. 4. Measurements of the cross section of the $e^+e^- \to Ze^+e^- \to q\bar{q}e^+e^-$ process as a function of the centre-of-mass energy. The WPHACT predictions are assigned an uncertainty of 5%. As reference, a line indicates the GRC4F expectations.

References

[1] DELPHI Collaboration, P. Abreu, et al., Phys. Lett. B 515 (2001) 238.
[2] ALEPH Collaboration, R. Barate, et al., Phys. Lett. B 462 (1999) 389;
ALEPH Collaboration, A. Heister, et al., Eur. Phys. J. C 21 (2001) 423;
DELPHI Collaboration, P. Abreu, et al., Phys. Lett. B 459 (1999) 382;
DELPHI Collaboration, P. Abreu, et al., Phys. Lett. B 502 (2001) 9;
L3 Collaboration, M. Acciarri, et al., Phys. Lett. B 403 (1997) 168;

L3 Collaboration, M. Acciarri, et al., Phys. Lett. B 436 (1998) 417;
L3 Collaboration, M. Acciarri, et al., Phys. Lett. B 487 (2000) 229;
L3 Collaboration, P. Achard, et al., Phys. Lett. B 547 (2002) 151.
[3] OPAL Collaboration, G. Abbiendi, et al., Phys. Lett. B 438 (1998) 391;
OPAL Collaboration, G. Abbiendi, et al., Eur. Phys. J. C 24 (2002) 1.
[4] L3 Collaboration, B. Adeva, et al., Nucl. Instrum. Methods A 289 (1990) 35;
O. Adriani, et al., Phys. Rep. 236 (1993) 1;
M. Chemarin, et al., Nucl. Instrum. Methods A 349 (1994) 345;
M. Acciarri, et al., Nucl. Instrum. Methods A 351 (1994) 300;
G. Basti, et al., Nucl. Instrum. Methods A 374 (1996) 293;
I.C. Brock, et al., Nucl. Instrum. Methods A 381 (1996) 236;
A. Adam, et al., Nucl. Instrum. Methods A 383 (1996) 342.
[5] WPHACT version 2.1;
E. Accomando, A. Ballestrero, Comput. Phys. Commun. 99 (1997) 270;
E. Accomando, A. Ballestrero, E. Maina, hep-ph/0204052.
[6] GRC4F version 2.1;
J. Fujimoto, et al., Comput. Phys. Commun. 100 (1997) 128.
[7] KK2f version 4.13;
S. Jadach, B.F.L. Ward, Z. Wąs, Comput. Phys. Commun. 130 (2000) 260.
[8] PHYTHIA version 5.772 and JETSET version 7.4;
T. Sjöstrand, CERN-TH/7112/93 (1993), revised 1995;
T. Sjöstrand, Comput. Phys. Commun. 82 (1994) 74.
[9] KORALW version 1.33;
M. Skrzypek, et al., Comput. Phys. Commun. 94 (1996) 216;
M. Skrzypek, et al., Phys. Lett. B 372 (1996) 289.
[10] F.A. Berends, R. Pittau, R. Kleiss, Comput. Phys. Commun. 85 (1995) 437.
[11] PHOJET version 1.05;
R. Engel, Z. Phys. C 66 (1995) 203;
R. Engel, J. Ranft, S. Roesler, Phys. Rev. D 52 (1995) 1459.
[12] F.A. Berends, P.H. Daverfeldt, R. Kleiss, Nucl. Phys. B 253 (1985) 441.
[13] The L3 detector simulation is based on GEANT 3.21, see R. Brun, et al., CERN report CERN DD/EE/84-1 (1984), revised 1987;
Uses GHEISHA to simulate hadronic interactions, see H. Fesefeldt, RWTH Aachen report PITHA 85/02 (1985).
[14] S. Bethke, et al., Nucl. Phys. B 370 (1992) 310, and references therein.